Electronic Spectra of the Cyclometalated Complexes M(2-thienylpyridine)$_2$ with M = Pd, Pt: A Theoretical Study

Kristine Pierloot* and Arnout Ceulemans

Chemistry Department, University of Leuven, Celestijnenlaan 200F, B-3001 Heverlee-Leuven, Belgium

Manuela Merchán and Luis Serrano-Andrés

Departamento de Química Física, Universitat de València, Dr. Moliner 50, Burjassot, E-46100 València, Spain

Received: September 21, 1999; In Final Form: February 22, 2000

The optical spectra of the cyclometalated complexes Pd,Pt(thpy)$_2$, with thpy$^-$, the deprotonated form of 2-(2-thienyl)pyridine, have been calculated using a multiconfigurational second-order perturbation treatment based on a complete active space reference wave function, i.e., the CASSCF/CASPT2 method. The calculations were performed on optimized structures within C_{2v} symmetry, obtained using density functional theory (DFT). The structure and lowest excited states of free protonated thpyH were also calculated. On the basis of the calculated results for excitation energies and oscillator strengths, the most important bands in the experimental absorption spectra of the complexes were assigned as excitations to states of symmetry $^1A_1$ or $^1B_2$, all of mixed charge-transfer/ligand-centered character. The lowest triplet excited state was calculated to be the a $^3A_1$ state, closely followed by the $^3B_2$ state. Both excitations were found to be almost purely ligand-centered, with a very limited charge-transfer contribution in Pd(thpy)$_2$ and an only slightly larger contribution in Pt(thpy)$_2$. The differences between the position and character of the singlet excited states in the absorption spectra of both molecules are also discussed. The results are found to be consistent with the trends obtained from previous experimental measurements.

1. Introduction

The photophysical and photochemical properties of transition metal compounds with organic ligands are determined by the characteristics of the lowest excited states. In most "traditional" metal compounds, the lowest excitations either are metal-centered (MC, the so-called ligand-field or d−d transitions) or are of charge-transfer character (metal-to-ligand (MLCT) or ligand-to-metal (LMCT)). During the past decade, however, a new class of compounds (the cyclometalated complexes) was described and characterized chemically, photochemically, and photophysically.[1,2] The investigations revealed that the lowest excited states in these complexes are largely ligand-centered (LC) of $\pi-\pi^*$ character, with a varying degree of MLCT admixture. This information was obtained from highly resolved emission and excitation spectra as well as from emission decay properties.[3−10] Theoretical insight into the nature of the excited states in these complexes has so far been limited to the general assignment of the states as belonging to one of the above categories.[11,12]

In this work we will describe and compare the absorption spectrum of two cyclometalated complexes, containing either Pd(II) or Pt(II) as the central metal coordinated to two cis-configured C-deprotonated 2-(2-thienyl)pyridine (thpy$^-$) ligands. The structural formula of the two complexes, which will further be referred to as Pd(thpy)$_2$ or Pt(thpy)$_2$ is shown in the following scheme.

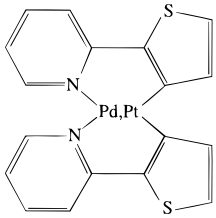

The absorption spectra of both complexes are calculated using multiconfigurational perturbation theory based on a complete active space reference wave function, i.e., the CASSCF/CASPT2 method.[13] This method has proven to be successful for the calculation of electronic spectra of more traditional inorganic and organometallic transition metal systems, where both metal-centered (MC) and charge-transfer (CT) excitations are described with an accuracy of 2500 cm^{-1} or better.[14−17] The complexes considered in this work present an additional challenge to the CASPT2 method. Indeed, as will be illustrated below, the success of the method critically depends on its ability to describe all states of interest with a number of "active" orbitals, which is with today's computer power limited to 12−14. This so-called active orbital space has to comprise all valence orbitals that either contain important (static) correlation effects or those involved (populated or depopulated) in any of the excited states. Since in the present complexes three different types of excitations, MC, (ML)CT, or LC, have to be described simultaneously, the choice of active orbitals will necessarily have to be economic, comprising, for example, only the HOMO−LUMO

* Fax: +32-16 32 79 92. E-mail: Kristin.Pierloot@chem.kuleuven.ac.be.

10.1021/jp993384s CCC: $19.00
Published on Web 04/18/2000

TABLE 1: Structural Data Obtained from BP86-DFT Geometry Optimizations on the Ground State of Pd(thpy)$_2$ and Pt(thpy)$_2$[a]

	Pd(2-thpy)$_2$		Pt(2-thpy)$_2$	
	C_{2v}	C_2	C_{2v}	C_2
R(M−C) (Å)	2.01	2.00	2.01	2.00
R(M−N) (Å)	2.24	2.20	2.25	2.21
C−M−C (deg)	97.1	97.3	99.2	99.7
C−M−N (deg)	80.3	80.7	79.0	79.4
N−M−N (deg)	102.4	103.9	102.8	103.6

[a] C, N are the coordinating atoms of the thpy$^-$ ligands; M = Pd, Pt.

thpy π pairs instead of the full valence π space that is customarily used for the description of the electronic spectra of organic molecules.[16,18,19] Even if these restrictions do afflict the present CASPT2 calculations with somewhat larger uncertainties, we will show that the calculated results are still accurate enough to characterize and assign the important electronic features in the UV−vis region of the experimental spectra of both molecules and to describe the differences between the Pd and Pt complex. No previous theoretical studies have been reported for the spectra of the present complexes. Their interpretation has so far been based only on experimental evidence and on qualitative theoretical considerations The present contribution therefore is the first in providing a detailed assignment of the spectra under consideration.

2. Computational Details

2.1. Geometry Optimizations. To provide the structures to be used for the calculation of the electronic spectra, a set of geometry optimizations was first performed on the neutral C-protonated thpyH ligand, both in its lowest singlet and triplet states, and on the Pd(thpy)$_2$ and Pt(thpy)$_2$ molecules in their singlet ground state. These structure optimizations were performed using density functional theory (DFT) with a BP86 (Becke−Perdew) functional,[20,21] making use of the Turbomole code.[22] The Coulomb integrals were treated with the resolution of identity (RI) approximation, using the default auxiliary basis sets included in Turbomole. Pd and Pt were treated with 28- and 60-electron relativistic effective core potentials from Andrae et al.,[23] combined with the Turbomole default SV(P) basis sets. SV(P) basis sets were also used for all other atoms.

The optimized structure of the free thpy ligand turned out to be completely flat, C_s symmetry, for both the lowest singlet state, ^{1}A′, and the lowest triplet, ^{3}A′. Also in Pd(thpy)$_2$ and Pt(thpy)$_2$ the two thpy$^-$ ligands essentially remain flat. However, they are rotated with respect to each other, by 18.6° in the palladium and 16.8° in the platinum compound. The optimum geometry of these molecules therefore has C_2 symmetry, not C_{2v}. The energy gain with respect to a flat structure, optimized by enforcing C_{2v} symmetry, is rather limited: 2.1 kcal/mol for Pd(thpy)$_2$, 1.7 kcal/mol for Pt(thpy)$_2$. The most important structural parameters resulting from the optimizations in C_2 and C_{2v} are shown in Table 1. Apart from the deviation from planarity in C_2, both structures are fairly similar, showing only a slight shortening of the metal−ligand bond distances in C_2 with respect to C_{2v}. For computational reasons, it was decided to perform the calculation of the absorption spectra of both molecules using the C_{2v} structures. The molecules were placed in the *yz* plane, such that σ-type orbitals are found in the representations a_1 and b_2, while π orbitals end up in b_1 and a_2.

2.2. Calculation of Electronic Spectra. The calculation of the absorption spectra was performed using the CASSCF/CASPT2 method,[13] as implemented in the MOLCAS.4.1 code.[24] For Pd and Pt the 30- and 62-electron relativistic core-AIMP (ab initio model potential) and corresponding [3s3p4d] valence basis sets of Barandiaran[25] and Casarrubios[26] were used. All other atoms were described using the ANO-S (atomic natural orbital) basis sets of Pierloot.[27] The latter were contracted to [3s2p1d] for the C and N bound to the metal, [3s2p] for all other C, [4s3p1d] for S, and [2s] for H. This leads to a total of 292 contracted basis functions. For the calculation of the free neutral thpyH, the basis set was enlarged to [3s2p1d] on all C in order to obtain a balanced description of this molecule.

The CASSCF/CASPT2 calculations consist of two major steps. In the first step, a CASSCF wave function is built by distributing a limited number of valence electrons over the so-called active orbital space. This active space should fulfill the following two requirements: (1) the resulting CASSCF wave function should include the most important correlation effects, and (2) orbitals involved in the excited states of interest should be included. In transition metal systems, important nondynamical correlation effects are found connected to covalent metal−ligand interactions.[16] To describe these effects, both the bonding and antibonding combination of metal and ligand orbitals have to be included in the CASSCF active space. In section 3.1 we will show that in the present case strongly covalent σ bonds are formed between Pd(II), Pt(II), and the formally negative thpy$^-$ ligands, and we will look in more detail at the active orbitals describing these interactions. Here, we only mention that the relevant orbitals are the bonding and antibonding combination of thpy σ (mainly centered on the C lone pairs) and Pd 4d$_{yz}$, Pt 5d$_{yz}$ in representation b_2, and of thpy σ and Pd 5s, Pt 6s in representation a_1. Orbitals involved in the low-lying excited states are (a) the remaining four 4,5 d orbitals ($2 \times a_1$, b_1, a_2) and (b) the HOMO−LUMO pair of thpy π orbitals ($2 \times b_1$, $2 \times a_2$). This gives a total of 12 active orbitals ($4 \times a_1$, $3 \times b_1$, $2 \times b_2$, $3 \times a_2$), populated with 16 electrons. Ideally, one would of course like to include in the active space all thpy π valence orbitals in order to get a better description of $\pi-\pi^*$ correlation effects and of the ligand centered excited states. This would, however, mean adding 14 more active orbitals, leading to an active space of 26 orbitals, which is far beyond the reach of today's computer power. To check the uncertainty on the excitation energies connected with the use of a limited thpy active space, test calculations on the lowest excited states of free C-protonated thpyH were performed with both a HOMO−LUMO (2 electrons in 2 orbitals) and a full valence π (12 electrons in 11 orbitals) active space. The results are presented in section 3.2.

In the CASPT2 step all electrons originating from Pd 4p, 4d, Pt 5p, 5d, C,N 2s, 2p, S 3s, 3p, and H 1s are correlated, resulting in a total number of 122 correlated electrons. As a result of limitations in the 12 orbital active space, quite strongly interacting intruder states appear in the CASPT2 calculations of some of the excited states. To deal with the intruders, the so-called LS-CASPT2 method[28,29] was employed, where the intruder states are dealt with by adding a level shift parameter to the zeroth order Hamiltonian combined with a level shift correction that should remove the effect of the level shift on the second-order energy. Test calculations with several level shift values were performed. The results are presented in the Appendix.

In almost all cases, the reference wave function of the CASPT2 calculation was built from individually optimized CASSCF orbitals for each of the excited states. However, in some cases this led to strongly overlapping states of the same

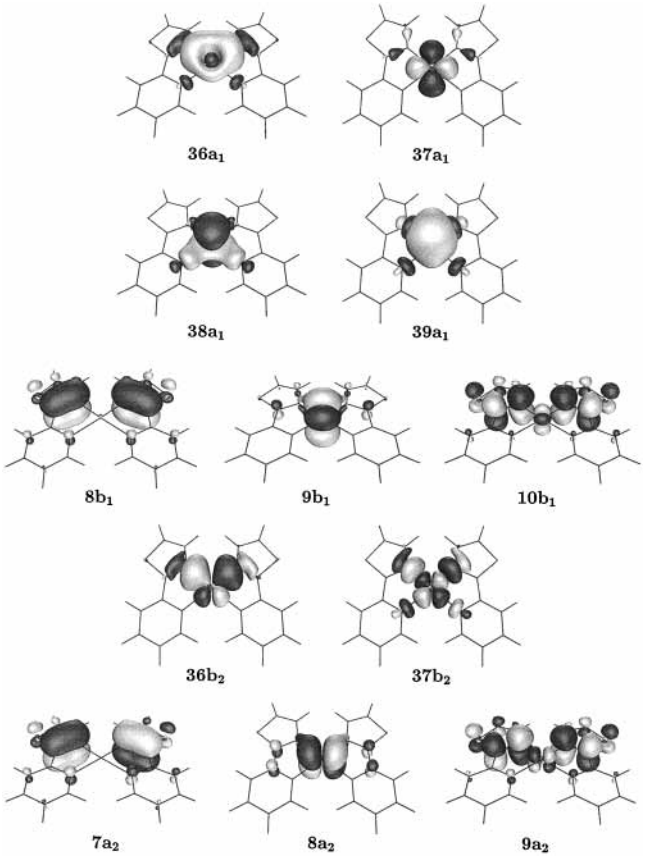

Figure 1. Active natural orbitals resulting from the CASSCF calculation on the X $^1A_1$ ground state of $Pt(thpy)_2$.

symmetry. This is, in particular, true for states of $^1A_1$ and $^1B_2$ symmetry, containing a mixture of CT and LC character. For those states, the reference wave function was instead obtained from a CASSCF calculation in which an average set of orbitals over the states of interest was optimized.

Finally, oscillator strengths were calculated by combining transition dipole moments obtained with the CASSI (CAS state interaction) approach[30] with CASPT2 excitation energies.

3. Results and Discussion

3.1. Electronic Structure of the Ground State. Information concerning the ground-state electronic structure in the considered complexes may be obtained from an inspection of the valence natural orbitals included in the CASSCF active space. In Figure 1, these orbitals are depicted for $Pt(thpy)_2$, while Table 2 shows the contributions (in terms of percentage) of the metal s, p, and d and thpy σ and π type orbitals to the ground-state active orbitals in both complexes. It should be noted that the numbering of the orbitals is not based on orbital energies (which are not defined for natural orbitals) but is (arbitrarily) chosen such that thpy $\sigma, \pi <$ metal $<$ thpy π^*. As such, the orbitals with formal metal d character are numbered $37,38a_1$, $9b_1$, $37b_2$, and $8a_2$.

The actual composition of these orbitals, in particular the extent of metal−ligand mixing, is illustrative of the degree of covalency of the metal−thpy interaction. The strongest covalency is found in representation b_2. Here we find the bonding ($36b_2$) and antibonding ($37b_2$) combination of thpy σ and metal d_{yz}, both molecular orbitals containing an almost equal contribution of metal and ligand character. The consequence of the strong admixture of d character into the bonding $36b_2$ orbital is that the d_{yz} orbital, formally empty in a Pd(II),Pt(II) d^8 ($d_\sigma^4 d_\pi^4$) configuration, in fact receives an appreciable electron count through σ-donation. The natural orbital occupation numbers in Table 2 also illustrate how this covalent metal−thpy interaction gives rise to important static correlation effects: the occupation numbers of $36b_2$ and $37b_2$ indeed significantly differ from 2 or 0, respectively. Some, but much less important covalent character is also found in the σ orbitals in representation a_1. Here we note in particular the strong admixture of thpy σ character into the metal 5,6s orbital. The orbital pair $36,39a_1$ is included in the active space in order to account for the correlation effects connected to this interaction.

Thpy to Pd, Pt σ-donation is to some extent counteracted by π-back-donation in the representations b_1 and a_2. As Figure 1 and Table 2 show, the orbitals $8b_1$ and $7a_2$ remain essentially pure thpy π in both complexes, and π-back-donation occurs by mixing between metal d and thpy π^* character in the couples $9,10b_1$ and $8,9a_2$. Whereas the extent of σ-donation is about the same in both complexes, giving rise to a d_σ occupation number of 4.85 in $Pd(thpy)_2$ and 4.84 in $Pt(thpy)_2$, the extent of admixture in the π orbitals; i.e., π-back-donation is slightly more important in $Pt(thpy)_2$: the number of ground-state d_π electrons is 3.80 for $Pd(thpy)_2$ and only 3.70 for $Pt(thpy)_2$. Summing up, this gives a total d electron count of 8.65 in the ground state of $Pd(thpy)_2$ and 8.54 in $Pt(thpy)_2$ (see also further in Tables 4 and 5).

3.2. Results for the 2-(2-Thienyl)pyridine Molecule. The results of the calculations performed for free neutral thpyH are shown in Table 3. Both the lowest singlet excited state, A $^1A'$ (vertical excitation), and the lowest triplet state, a $^3A'$ (vertical absorption, 0−0 excitation and vertical emission) are included.[31] Experimentally, the absorption spectrum of thpyH shows a strong band at 33 113 cm^{-1}, while the emission spectrum ranges from 16 600 to 20 600 cm^{-1}].[1,11]

The energy difference between the CASPT2 results obtained starting either from a valence π CASSCF (PT2B) or a minimal (2 in 2) CASSCF wave function (PT2A) can be considered a measure of the errors to be expected for the excitation energies of the ligand-centered LC and charge-transfer (ML)CT states in the Pd and Pt complexes. Somewhat surprisingly, the sign of the error is different for the lowest singlet and triplet state. For the $^3A'$ state we find that the PT2A calculations systematically overestimate the excitation energy, by 700−1500 cm^{-1}. On the other hand, the excitation energy of the A $^1A'$ state is considerably underestimated, by 2700 cm^{-1}, at the PT2A level of calculation. The result obtained for the latter excitation by PT2B, 33 147 cm^{-1}, nicely corresponds to the lowest absorption maximum in the experimental spectrum. The calculated results for the $^3A'$ phosphorescence maximum and 0−0 transition energy span the energy range of emission bands in the phosphorescence spectrum, although the calculated 0−0 transition energy is about 1000 cm^{-1} lower than the highest energy recorded at 20 600 cm^{-1}.[1,11] Finally, it is also worth mentioning the good performance of the BP86-DFT approach for the relative location of the lowest triplet state with respect to the ground state, yielding results at about 400 cm^{-1} above the PT2B findings. Unfortunately, standard DFT calculations are restricted to the lowest state of a certain spin and symmetry and the method could therefore not be applied for the lowest excited singlet state of free thpyH (of the same symmetry as the ground state), nor for the calculation of the spectra of the Pd and Pt complexes. Such calculations can, however, be performed using the time-dependent DFT formalism, which has already been proven to be successful in some transition metal complexes[32] and may therefore offer an alternative for the present CASPT2 treatment of the complexes under consideration.

TABLE 2: Composition of the Ground State Active Orbitals in Pd,Pt(thpy)$_2$, Obtained from a Mulliken (gross) Analysis[a]

	Pd(thpy)$_2$						Pt(thpy)					
		Pd			thpy			Pt			thpy	
orbital	occ no.	s	p	d	σ	π	occ no.	s	p	d	σ	π
36a$_1$	1.965	13.6	0.0	4.8	81.6		1.970	7.5	1.0	10.1	81.4	
37a$_1$	2.000	0.2	0.0	97.5	2.3		2.000	0.6	0.0	95.8	3.6	
38a$_1$	1.994	7.0	0.0	88.9	4.1		1.997	9.4	0.0	77.	13.7	
39a$_1$	0.024	35.1	3.5	10.9	49.5		0.024	24.2	1.8	12.7	61.3	
8b$_1$	1.945		0.4	−1.3		101.1	1.946		0.6	−1.7		101.1
9b$_1$	1.995		0.0	92.2		7.8	1.995		0.0	89.6		10.4
10b$_1$	0.063		−0.9	2.2		98.7	0.061		−0.8	2.6		98.2
36b$_2$	1.939		−0.4	42.5	57.9		1.957		0.0	37.6	62.4	
37b$_2$	0.076		−1.1	53.2	47.9		0.050		−1.3	53.9	47.4	
7a$_2$	1.945			−0.6		100.6	1.946			−1.7		101.7
8a$_2$	1.993			91.7		8.3	1.993			89.2		10.8
9a$_2$	0.062			3.3		96.7	0.060			4.1		95.9

[a] The (small) negative numbers in the table are due to the equal distribution of the (negative) overlap between the contributing atomic orbitals in a Mulliken gross composition analysis; they are an artifact and have no physical meaning.

TABLE 3: Calculated Excitation Energy (cm^{-1}) with Different Methods (see text) for the Lowest Singlet and Triplet Excited States in Neutral ThpyH

final state[31]	method[a]	vertical excitation	0−0 transition energy	phosphorescence max.
a ^{3}A′	PT2A	23 691	19 921	17 179
	PT2B	22 137	19 196	16 453
	DFT	22 509	19 610	16 855
A ^{1}A′	PT2A	30 468		
	PT2B	33 147		
exp emission:[1,11] 16 600−20 600 cm^{-1}				
exp abs max.:[1,11] 33 113 cm^{-1}				

[a] PT2A = CASPT2 based on a (2 in 2) CASSCF wave function; PT2B = CASPT2 based on a valence π (12 in 11) CASSCF wave function.

3.3. Characterization of the Excited States. The spectroscopic properties of transition metal complexes are usually discussed with the assumption that the ground state as well as the excited states can be described in a sufficiently approximate way by localized molecular orbital configurations. Only with this assumption can the spectroscopic transitions be classified as being metal-centered (MC) or ligand-centered (LC) or having charge-transfer (CT) character. In section 3.1 we have already seen that, at least as the MC transitions are concerned, such a classification can in the considered complexes not be strictly made. Indeed, as indicated by Figure 1 and Table 2, the formal Pd 4d,Pt 5d orbital 37b$_2$ in fact contains an almost equal mixture of metal 4,5d and thpyσ character. Since this is the orbital receiving an electron in all so-called metal-centered (MC) excitations, it should be clear that the latter in fact also contains a significant contribution of metal-to-ligand charge-transfer character. As we will see further, the characterization of some of the other excited states as either LC or CT is even more fuzzy. Even so, we have, for the sake of simplicity, tried to maintain some classification of the different excited states into MC, LC, and CT in Tables 4 and 5 and the rest of the discussion. Please note that in what follows CT always stands for MLCT, since only metal d to thpy π* charge-transfer excitations, but no thpy π to metal d excitations, were found in the calculated region of the spectra.

The results obtained from the CASSCF/CASPT2 calculations on all low-lying (up to 45 000−50 000 cm^{-1}) triplet and singlet excited states in Pd(thpy)$_2$ and Pt(thpy)$_2$ are shown in Tables 4 and 5, respectively. The tables include the composition in terms of single excitations of all states, and the classification in terms of MC, LC, or CT is based on the character of the orbitals involved in the principal singly excited configuration. It should be stressed however that, even if we have used the same labeling of the orbitals in Tables 4 and 5 as in Table 2 and Figure 1, indicating that the main character of these orbitals is indeed the same, the exact composition of the orbitals involved in the excitations may in some cases be thoroughly different from the corresponding ground-state orbitals. This is due to the fact that individual orbital CASSCF optimizations were performed for each of the excited states (with a few exceptions, see section 2), allowing the relevant orbitals to relax from a shape that is optimal for ground-state correlation to a shape that is adapted to the new excited-state configuration. In practice, this means, for example, that the thpy π* orbitals get more localized on the five-rings instead of only on the six-rings (see Figure 1), while for some excited LC and CT states we also find considerably more mixing between the metal d and thpy π* orbitals in the 9,10b$_1$ and 8,9a$_2$ couples.

A more detailed picture of the electron charge-transfer involved in each of the excited states is provided by Figure 2 and Tables 4 and 5. Figure 2 pictures the changes in electron density for a number of relevant excited states as compared to the ground state in Pt(thpy)$_2$, while the numbers at the right side of Tables 4 and 5 list the total number of metal d electrons, subdivided in d$_\sigma$ and d$_\pi$, obtained from a Mulliken population analysis of the different states in both complexes. The first two plots in Figure 2 are typical for MC excitations. One can see the reorganization of electron density within the Pt 5d shell, from d$_\pi$ to d$_\sigma$ in the B ^{1}A$_2$ state and from d$_\sigma$ to d$_\sigma$ in the D ^{1}B$_2$ state, together with a transfer of electron density into the lone pairs on the coordinating C and N atoms of the thpy$^-$ ligands. The corresponding populations in Tables 4 and 5 show that the total metal d population indeed decreases in all MC excited states as compared to the ground state, by 0.19−0.35 e in Pd(thpy)$_2$ and by 0.15−0.33 e in Pt(thpy)$_2$.

The electron density changes in the CT excited states of symmetry ^{1,3}B$_1$ and ^{1,3}A$_2$ also show a typical pattern. An example is the state A ^{1}B$_1$ shown in Figure 2. The principal single electron excitation is for all these states from a metal d$_\sigma$ orbital (37,38a$_1$) into a thpy π* orbital (10b$_1$,9a$_2$). However, as can be seen from the density difference plot, the metal d$_\sigma$ → thpy π* electron flow is to some extent counteracted by an opposite flow out of the σ lone pairs on the thpy C,N. This explains why the actual decrease in metal d population for these CT states is considerably less than one. From Tables 4 and 5 we find metal d populations ranging between 8.05 and 8.34 for

TABLE 4: Calculated Spectrum of Pd(2-thpy)$_2$ at the CASSCF and CASPT2 Levels (cm^{-1})

	exc. energy(osc. str.)					Pd d population[b]		
final state[31]	CASSCF	CASPT2		type[a]	single excitation	d_σ	d_π	total
X $^1A_1$						4.85	3.80	8.65
a $^3A_1$	30 903	19 689		LC	$8b_1 \rightarrow 10b_1$(56%); $7a_2 \rightarrow 9a_2$(35%)	4.86	3.76	8.62
a $^3B_2$	30 784	19 957		LC	$7a_2 \rightarrow 10b_1$(57%); $8b_1 \rightarrow 9a_2$(34%)	4.86	3.77	8.63
A $^1A_1$	41 665	24 432	(0.0306)	CT	$9b_1 \rightarrow 10b_1$(82%)	5.12	3.1	8.25
A $^1B_2$	43 513	26 052	(0.1994)	CT	$8a_2 \rightarrow 10b_1$(86%)	5.11	3.18	8.29
a $^3B_1$	35 270	26 411		CT	$38a_1 \rightarrow 10b_1$(89%)	4.45	3.85	8.30
b $^3B_2$	28 341	27 486		MC	$38a_1 \rightarrow 37b_2$(92%)	4.57	3.85	8.42
A $^1B_1$	3325	27 960	(0.0298)	CT	$38a_1 \rightarrow 10b_1$(89%)	4.41	3.86	8.27
c $^3B_2$	46 019	28 541		CT	$8a_2 \rightarrow 10b_1$(52%); $9b_1 \rightarrow 9a_2$(33%)	5.16	3.05	8.21
a $^3A_2$	30 643	29 169		MC	$9b_1 \rightarrow 37b_2$(91%)	5.40	2.92	8.32
b $^3A_1$	46 292	30 385[c]		CT	$9b_1 \rightarrow 10b_1$(52%); $8a_2 \rightarrow 9a_2$(33%)	5.14	3.11	8.25
b $^3B_1$	31 761	30 675		MC	$8a_2 \rightarrow 37b_2$	5.39	2.9	8.32
B $^1B_2$	52 648	31 240	(0.0324)	LC	$7a_2 \rightarrow 10b_1$(73%); $38a_1 \rightarrow 37b_2$(9%)	4.93	3.47	8.40
b $^3A_2$	41 636	31 371		CT	$38a_1 \rightarrow 9a_2$(88%)	4.49	3.85	8.34
A $^1A_2$	42 071	31 745		CT	$38a_1 \rightarrow 9a_2$(88%)	4.44	3.86	8.30
B ^1A	55 392	32 022[c]	(0.2985)	LC	$8b_1 \rightarrow 10b_1$(74%)	4.97	3.44	8.41
C $^1B_2$	48 692	32 163	(0.0847)	CT	$9b_1 \rightarrow 9a_2$(83%)	5.22	3.06	8.28
B $^1A_2$	36 692	33 127		MC	$9b_1 \rightarrow 37b_2$(89%)	5.51	2.95	8.46
d $^3B_2$	52 154	33 205[c]		CT	$38a_2 \rightarrow 10b_1$(37%); $9b_1 \rightarrow 9a_2$(46%)	5.13	3.09	8.22
D $^1B_2$	38 909	33 342	(0.0466)	MC	$38a_1 \rightarrow 37b_2$(90%)	4.63	3.83	8.46
e $^3B_2$	31 576	33 605		MC	$37a_1 \rightarrow 37b_2$(91%)	4.49	3.82	8.31
B $^1B_1$	37 975	34 397	(0.0011)	MC	$8a_2 \rightarrow 37b_2$(88%)	5.48	2.98	8.46
c $^3A_1$	52 510	34 692[c]		CT	$9b_1 \rightarrow 10b_1$(29%); $8a_2 \rightarrow 9a_2$(55%)	5.15	3.05	8.20
c $^3B_1$	47 545	37 151		CT	$37a_1 \rightarrow 10b_1$(82%); $8a_2 \rightarrow 37b_2$(6%)	4.38	3.67	8.05
C $^1B_1$	47 200	37 526	(0.0002)	CT	$37a_1 \rightarrow 10b_1$(89%)	4.30	3.83	8.13
E $^1B_2$	39 108	37 588	(0.0014)	MC	$37a_1 \rightarrow 37b_2$(91%)	4.55	3.84	8.39
C $^1A_2$	52 869	41 739		CT	$37a_1 \rightarrow 9a_2$(81%); $9b_1 \rightarrow 37b_2$(7%)	4.41	3.77	8.18
c $^3A_2$	53 464	41 881		CT	$37a_1 \rightarrow 9a_2$(88%)	4.33	3.83	8.16

[a] For the definition of MC, LC, and CT, see text. [b] From Mulliken population analysis. [c] Calculated with a level shift of 0.3 au (for all other states a level shift of 0.2 au was used): see Appendix.

TABLE 5: Calculated Spectrum of Pt(2-thpy)$_2$ at the CASSCF and CASPT2 Levels (cm^{-1})

	exc. energy(osc. str)					Pt d population[b]		
final state[31]	CASSCF	CASPT2		type[a]	single excitation	d_σ	d_π	total
X $^1A_1$						4.84	3.70	8.54
a $^3A_1$	30 055	18 168		LC	$8b_1 \rightarrow 10b_1$(61%); $7a_2 \rightarrow 9a_2$(31%)	4.87	3.62	8.49
a $^3B_2$	30 057	18 829		LC	$7a_2 \rightarrow 10b_1$(61%); $8b_1 \rightarrow 9a_2$(32%)	4.86	3.65	8.51
A $^1A_1$	38 227	20 441	(0.0116)	CT	$9b_1 \rightarrow 10b_1$(82%)	5.07	3.02	8.09
A $^1B_2$	42 466	23 454	(0.2342)	CT	$8a \rightarrow 10b_1$(88%)	5.09	3.01	8.10
a $^3B_1$	33 517	24 856		CT	$38a_1 \rightarrow 10b_1$(93%)	4.34	3.77	8.11
b $^3B_2$	43 839	24 930		CT	$9b_1 \rightarrow 9a_2$(46%); $8a_2 \rightarrow 10b_1$(44%)	5.10	2.99	8.09
b $^3A_1$	44 696	26 116[c]		CT	$8a_2 \rightarrow 9a_2$(49%); $9b_1 \rightarrow 10b_1$(40%)	5.08	3.06	8.14
B $^1B_2$	47 575	26 397	(0.0268)	CT	$9b_1 \rightarrow 9a_2$(85%); $7a_2 \rightarrow 10b_1$(3%)	5.10	3.01	8.12
A $^1B_1$	35 846	26 550	(0.0340)	CT	$38a_1 \rightarrow 10b_1$(92%)	4.33	3.78	8.11
c ^3B	51 182	28 284[c]		CT	$8a_2 \rightarrow 10b$(40%); $9b_1 \rightarrow 9a_2$(37%)	5.02	3.12	8.14
c $^3A_1$	51 311	29 214[c]		CT	$8a_2 \rightarrow 9a_2$(51%); $9b_1 \rightarrow 10b_1$(37%)	5.07	3.03	8.10
C $^1B_2$	53 779	29 718	(0.0173)	LC	$7a_2 \rightarrow 10b_1$(73%); $9b_1 \rightarrow 9a_2$(2%)	4.95	3.32	8.27
B $^1A_1$	54 762	31 010[c]	(0.3038)	LC	$8b_1 \rightarrow 10b_1$(73%)	4.95	3.30	8.25
a $^3A_2$	41 313	31 180		CT	$38a_1 \rightarrow 9a_2$(92%)	4.37	3.79	8.16
A $^1A_2$	41 512	31 390		CT	$38a_1 \rightarrow 9a_2$(92%)	4.35	3.80	8.15
b $^3A_2$	36 165	32 864		MC	$9b_1 \rightarrow 37b_2$(91%)	5.40	2.84	8.24
B $^1B_1$	44 964	34 101	(0.0008)	CT	$37a_1 \rightarrow 10b_1$(92%)	4.23	3.74	7.97
b $^3B_1$	44 945	34 197		CT	$37a_1 \rightarrow 10b_1$(92%)	4.23	3.75	7.98
d $^3B_2$	35 793	34 400		MC	$38a_1 \rightarrow 37b_2$(92%)	4.58	3.77	8.35
c $^3B_1$	37 702	34 956		MC	$8a_2 \rightarrow 37b_2$(91%)	5.39	2.86	8.25
B $^1A_2$	42 026	36 764		MC	$9b_1 \rightarrow 37b_2$(89%)	5.46	2.88	8.34
D $^1B_2$	40 950	38 147	(0.0367)	MC	$38a_1 \rightarrow 37b_2$(92%)	4.63	3.76	8.39
C $^1B_1$	43 662	38 548	(0.0022)	MC	$8a_2 \rightarrow 37b_2$(88%)	5.45	2.93	8.38
e $^3B_2$	41 763	38 853		MC	$37a_1 \rightarrow 37b_2$(92%)	4.48	3.73	8.21
c $^3A_2$	51 483	39 432		CT	$37a_1 \rightarrow 9a_2$(91%)	4.24	3.76	8.00
C $^1A_2$	51 527	39 518		CT	$37a_1 \rightarrow 9a_2$(90%)	4.25	3.76	8.01
E $^1B_2$	45 805	42 738	(0.0005)	MC	$37a_1 \rightarrow 37b_2$(92%)	4.52	3.74	8.26

[a] For the definition of MC, LC and CT: see text. [b] From Mulliken population analysis. [c] Calculated with a level shift of 0.3 au (for all other states a level shift of 0.2 au was used): see Appendix.

Pd and between 7.97 and 8.16 for Pt, i.e., a decrease of at most 0.6 electron with respect to the ground state.

The characterization of the lowest excited triplet state in both spectra has conceived considerable attention in recent experimental literature.[2−5,7] On the basis of highly resolved excitation and emission spectra in Shpol'skii matrixes this state was classified as being ligand-centered with a relatively small (in Pd(thpy)$_2$) to considerable (in Pt(thpy)$_2$) MLCT admixture. This

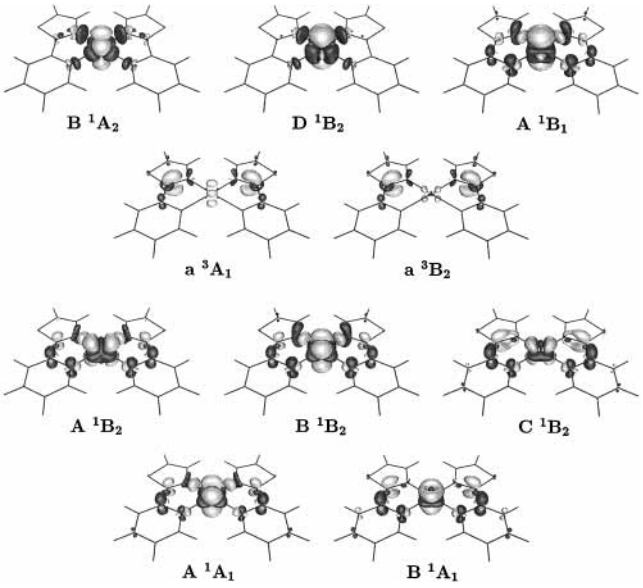

Figure 2. Plots of the electron density difference (obtained at the CASSCF level) between a number of representative excited states and the ground state in $Pt(thpy)_2$.

conclusion was, among other arguments (see also section 3.4), reached from an analysis of the zero-field splitting of this triplet state, which was found to be very small (<1 cm^{-1}) for $Pd(thpy)_2$, but considerably larger, 16 cm^{-1}, for $Pt(thpy)_2$. Our calculations confirm the assignment as LC for the lowest a $^3A_1$ state and also for the second a $^3B_2$ state. In fact, very little CT admixture is found for these states. This can be seen from Figure 2, showing only a small negative feature in the Pt region and some reorganization of electron density in the thpy π orbitals. From Tables 4 and 5 it can be seen that the metal d population is for these states very close to the ground-state population. Some CT admixture can be deduced from the reduction in d_π population, which is indeed slightly larger (0.03−0.05 e) in $Pt(thpy)_2$ than in $Pd(thpy)_2$ (0.02−0.03 e). With such a small difference in CT admixture, one might suppose that the larger zero-field splitting of the lowest LC state in the Pt complex should be essentially brought back to the intrinsically more important spin−orbit coupling in Pt than in Pd. Spin−orbit coupling has not been considered in the present calculations but will be the subject of further investigation.

Considerably more severe mixing between LC and CT character is found from our calculations for the singlet excited states of symmetry A_1 and B_2. The electron density difference plots corresponding to all calculated states of these symmetries in $Pt(thpy)_2$ have been included in Figure 2. As one can see, all excitations are accompanied by a pronounced reorganization of electron density both around the metal and in the thpy π region. On the basis of the populations in Tables 4 and 5 the states B $^1A_1$ and C $^1B_2$ have been classified as LC in $Pt(thpy)_2$, while for $Pd(thpy)_2$ the corresponding states are B $^1A_1$ and B $^1B_2$. We indeed find a significantly larger metal d population for these two states (8.40−8.41 in $Pd(thpy)_2$; 8.25−8.27 in $Pt(thpy)_2$) than for the CT states of the same symmetry (8.25−8.29 in $Pd(thpy)_2$; 8.09−8.12 in $Pt(thpy)_2$). However, these numbers also show that the separation between LC and CT is for these states really made up by a thin line. We also note that the admixture of CT character in the LC states is larger in $Pt(thpy)_2$ than in $Pd(thpy)_2$, with 0.27−0.28 e transferred from Pt d to thpy π^* orbitals in the former and 0.24−0.25 e from Pd d to thpy π^* in the latter complex.

3.4. Comparison with Experimental Spectra. The calculated excitation energies and corresponding oscillator strengths of the different excited states in $Pd(thpy)_2$ and $Pt(thpy)_2$ are reported in Tables 4 and 5, respectively. These data may be used to provide an explanation for the observed electronic spectra of both complexes and to discuss some trends between $Pd(thpy)_2$ and $Pt(thpy)_2$.

From highly resolved excitation and emission spectra the electronic origin, i.e., the 0−0 transition, of the lowest excited triplet state was established at 18 418 cm^{-1} in $Pd(thpy)_2$[3] and 17 156 cm^{-1} in $Pt(thpy)_2$,[5] i.e., 2100 and 3400 cm^{-1} below the corresponding transition energy in the free neutral thpyH ligand.[33] This sequence, together with the increased zero-field splitting in the Pt complex, as well as the decreased emission lifetime of the triplet state and the increased ratio of metal−ligand vibrational satellites relative to all vibrational satellites in the latter complex, has led to the conclusion that the extent of CT admixture must be considerably larger in $Pt(thpy)_2$ than in $Pd(thpy)_2$.[5] The extent of CT admixture in the lowest triplet states has been discussed in section 3.3. Here we note that, consistent with experiment, the calculated excitation energies of the a $^3A_1$ and a $^3B_2$ states are about 1500 cm^{-1} lower for $Pt(thpy)_2$ (18 168, 18 829 cm^{-1}) than for $Pd(thpy)_2$ (19 689, 19 957 cm^{-1}), both being considerably lower than the calculated vertical excitation energy for the free thpy ligand (22 137−23 691 cm^{-1}; see Table 3). Furthermore, the calculated (vertical) excitation energies are, as they should be, higher than the experimental 0−0 transition energy. Vertical excitation energies are energies of the excited states at the ground state geometry. In highly resolved absorption spectra they correspond to transitions to multiply excited vibrational levels at the high-energy side of the zero-phonon line. Also note that our calculations predict a significantly larger a $^3B_2$−a $^3A_1$ energy splitting in $Pt(thpy)_2$ than in $Pd(thpy)_2$, 661 versus 268 cm^{-1}.

Much less detailed information is available from experiment for the higher energy states. Room temperature absorption spectra were recorded (between 250 and 450 nm) for both complexes in different solutions,[11,12] where they show a series of broad bands. The most intense bands in both spectra, found below 340 nm ($>29\,000$ cm^{-1}), have been assigned as metal-perturbed LC transitions, since the lowest absorption band of the C-protonated thpyH ligand appears in the same region (see section 3.2). For $Pd(thpy)_2$, this region of the spectrum shows a maximum at 34 300 cm^{-1} with a shoulder at 31 200 cm^{-1}. In $Pt(thpy)_2$ the maximum is shifted to slightly lower energy, 33 000 cm^{-1}, while two shoulders are now found at around 30 800 and 28 000 cm^{-1} respectively. These data are to some extent solvent dependent:[1] differences of around 1000 cm^{-1} were observed for $Pt(thpy)_2$ between the band maxima in nitrile and cyclohexane solutions.[11] The neglect of chromophore−solvent interactions in our theoretical calculations might of course give rise to deviations between the calculated and experimental band maxima of at least this magnitude, and the comparison between the theoretical gas phase results and the experimental spectra should therefore be cautiously carried out. Our calculations indicate that the most intense band in both spectra should be assigned as the transition to the B $^1A_1$ state. This excitation indeed has the highest calculated oscillator strength. It is calculated at 32 022 cm^{-1} in $Pd(thpy)_2$ and 31 010 cm^{-1} in $Pt(thpy)_2$, about 2000 cm^{-1} lower than the experimental band maximum. This error can be brought back to the limitations in the CASSCF active space (see Table 3 and section 3.2), to the uncertainties connected with the use of a level shift (see the Appendix), and to the neglect of solvent effects. Our calculations

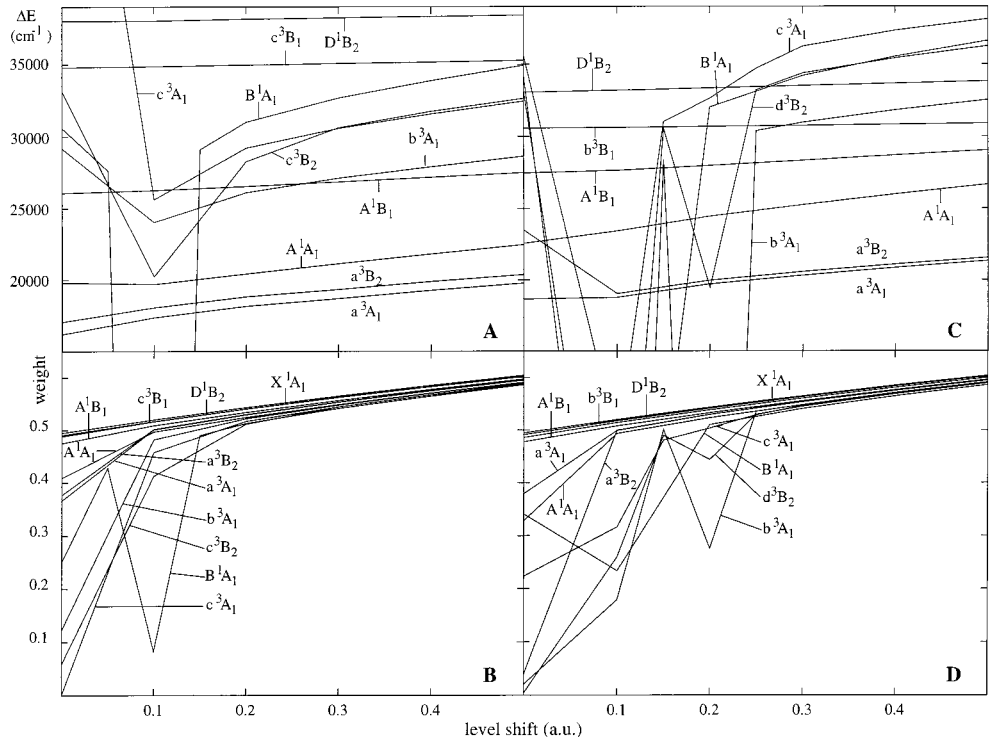

Figure 3. Plot of the level shift corrected CASPT2 excitation energy of a number of representative excited states as a function of the applied level shift in $Pt(thpy)_2$ (A) and $Pd(thpy)_2$ (C). The lower diagrams give the corresponding weights of the CASSCF reference wave function in $Pt(thpy)_2$ (B) and $Pd(thpy)_2$ (D).

do confirm the observed sequence in absorption energies between both complexes. We also classify the transition to B $^1A_1$ as mainly ligand-centered, but with a considerable CT admixture (see section 3.3 and Figure 3). As concerns the shoulders at the low-energy side of the B $^1A_1$ state, the CASPT2 results are less conclusive. The states B $^1B_2$ in $Pd(thpy)_2$ and C $^1B_2$ in $Pt(thpy)_2$, both also predominantly LC, are certainly good candidates. They are calculated about 1000 cm^{-1} below the B $^1A_1$ state with a considerably lower oscillator strength and are most probably responsible for the shoulder at 31 200 cm^{-1} in the $Pd(thpy)_2$ and at 30 800 cm^{-1} in the $Pt(thpy)_2$ spectrum. However, for the latter complex the calculated results predict two rather intense CT excitations at around 26 500 cm^{-1}, to B $^1B_2$ and A $^1B_1$, both of which could be responsible for the shoulder at 28 000 cm^{-1} in the experimental spectrum. On the other hand, for $Pd(thpy)_2$ the transition to A $^1B_1$ is calculated at 27 960 cm^{-1}, in a region with no obvious band in the experimental spectrum.

In the region above 340 nm both experimental absorption spectra show a second maximum with a shoulder at its low-energy side. In $Pd(thpy)_2$ the maximum is observed 26 300 cm^{-1} with a shoulder at 25 000 cm^{-1}. In $Pt(thpy)_2$, both bands are again shifted to lower energy: 23 900 and 21 700 cm^{-1} respectively. The calculated CASPT2 excitation energies offer a conclusive assignment of these two features, as the lowest singlet excited states of A_1, B_2 symmetry. For both complexes, the excitation to the A $^1B_2$ state is calculated highest in energy and with a considerably larger oscillator strength than the excitation to A $^1A_1$, and the latter should therefore be assigned to the low-energy shoulder, the former to the maximum. Both transitions have been classified as CT, and again the CASPT2 results confirm the observed trends in excitation energies between both complexes.

While the CT and LC states thus appear at a significantly lower energy in the absorption spectrum of $Pt(thpy)_2$ than in $Pd(thpy)_2$, the opposite is true for the MC states. All eight possible single MC excitations (four triplet, four singlet) have been included in our calculations. As can be seen from Tables 4 and 5, they range between 27 000 and 37 000 cm^{-1} in $Pd(thpy)_2$, and from 30 300 to 43 000 cm^{-1} in $Pt(thpy)_2$. It is noticeable that no MC transition is calculated below the dominating LC bands at around 32 000 cm^{-1} in the $Pt(thpy)_2$ spectrum, thus indicating that any MC excitation should be completely absent from the latter spectrum. For $Pd(thpy)_2$, only triplet but no singlet MC states are predicted to appear in the UV−vis region. The appearance of MC states at lower energies in the Pd spectrum is consistent with the general lower ligand field strength of Pd(II) as compared to Pt(II).[34] It is also confirmed by experimental temperature dependence studies of the luminescence lifetime of both complexes,[35] showing a persisting luminescence at room temperature in $Pt(thpy)_2$ but not in $Pd(thpy)_2$, due to the presence in the latter complex of distorted MC excited states that can be populated via a thermally activated radiationless transition.

4. Conclusion

In the present contribution we have demonstrated that it is today possible to obtain a quite accurate picture of the electronic spectrum of two large and complex transition metal systems, $Pd,Pt(thpy)_2$, using ab initio methods. Even if, due to the compelling use of a limited active space and the appearance of intruder states in the perturbation treatment, the presently reported CASPT2 results are afflicted with considerable uncertainties, the results are accurate enough to provide an assignment of the most important bands in the experimental absorption spectra of both molecules.

The character of the different excited states has been analyzed in detail and all of them have been classified as either MC, LC, or (ML)CT. It was, however, also shown that such a classification is not always unambiguous. In particular, considerable mixing between CT and LC character was found for the singlet excited states of A_1 and B_2 symmetry. On the other hand,

the excitations to the two lowest triplet states, a $^3A_1$ and a $^3B_2$, were found to be of almost pure LC character. In the case of $Pt(thpy)_2$ this seems to contradict some of the experimental findings.

As concerns the position of the excited states, our calculations nicely reproduce the trends between $Pd(thpy)_2$ and $Pt(thpy)_2$ suggested from experiment, i.e., the lower energy of the LC and CT states in $Pt(thpy)_2$ as compared to $Pd(thpy)_2$ and the lower energy of all MC states in the latter molecule.

Acknowledgment. This investigation has been supported by grants from the Flemish Science Foundation (FWO), the Concerted Research Action of the Flemish Government, and by the European Commission through the TMR program (grant ERBFMRXCT960079).

Appendix: Test Calculations with Different Level Shifts

Because of the use of a limited CASSCF active space, intruder states appeared in the subsequent perturbation treatment of the spectra reported in this work. Such intruder states frequently occur in CASPT2 calculations of electronic spectra of transition metal complexes and organic molecules.[29] To deal with them, a level-shift technique was developed,[28] making use of a level shift operator that modifies the zeroth-order Hamiltonian, together with a back-correction to the second-order energy. The LS-CASPT2 technique is, however, only truly successful in cases where the intruder states are only weakly interacting with the reference wave function. Successful means that the level shift effectively deals with the intruder states, but that in those regions of the applied level shift where no such intruders appear the calculated energies are not affected. As will be illustrated below, this requirement is not always fulfilled in the present calculations. We will show that for some excited states, the calculated excitation energy is quite strongly dependent on the actual value of the applied level shift, even if the latter value is large enough to deal with all intruder states. This is an indication that for these states some intruders are in fact strongly interacting with the reference state, and should ideally be moved into the CAS CI space. However, since the CASSCF active space used in the present calculations is at the limit of what can be treated with today's computer power, we necessarily have to settle for the LS-CASPT2 solution, while accepting the uncertainty on the calculated excitation energies as an additional source of error.

Test calculations with level shifts ranging between 0.0 and 0.5 au were performed for all states in both $Pt(thpy)_2$ and $Pd(thpy)_2$. The results obtained for a number of representative cases are shown in Figure 3. Parts A and C of Figure 3 show the calculated excitation energies as a function of the applied level shift for $Pt(thpy)_2$ and $Pd(thpy)_2$ respectively, while parts B and D of Figure 3 show the corresponding weights of the CASSCF reference in the final CASPT2 wave function. These weights give a measure of how large a fraction of the wave function is treated variationally in the CASSCF wave function and how much is treated by perturbation theory. A prerequisite for the CASPT2 method to provide a balanced treatment for relative energies is that the fraction of the wave function treated by CASSCF is approximately the same for all states involved. As one can see from Figure 3, this is the case for the results obtained at higher ($>0.2-0.3$ au) level shifts. At low level shifts, the weights for some of the excited states are considerably lower than the corresponding ground state weight and show strong oscillating behavior at values of the level shift where intruder states appear. The latter are accompanied by sudden drops in the calculated excitation energies, which often even become negative.

When looking in more detail at the different states included in Figure 3, we notice that all problematic states belong to either symmetry representation A_1 or B_2. Furthermore, the character of these states (see Tables 4 and 5) is either LC or CT. Indeed, no intruder state problem was met for any of the MC states, which therefore might just as well be calculated without level shift. Two representative cases are included in Figure 3: c $^3B_1$ and D $^1B_2$ for $Pt(thpy)_2$, b $^3B_1$ and D $^1B_2$ for $Pd(thpy)_2$. As one can see, the weights of these states remain close to the ground state weight at all level shifts, while the corresponding excitation energy shows a straight line with a virtually zero slope. Slightly worse but still satisfactory behavior is found for the CT states of symmetry A_2 and B_1, with A $^1B_1$ shown as a representative case in Figure 3. No intruders are found for these states either. However, the calculated excitation energies are not completely indifferent from the applied level shift: here, a straight line is found with a positive slope of about 3000 cm^{-1}/au. The implication of this is that the LS-CASPT2 results are not unique, but rather depend on a choice for the applied level shift. The recommended option is in such cases to select the lowest possible level shift that corrects the intruder state problems.[29] From the weights for $Pt(thpy)_2$ (Figure 3B) it would seem like a level shift of 0.2 au is appropriate. However, at this point, four of the energy curves, i.e., b,c $^3A_1$, B $^1A_1$, and c $^3B_2$, still show a significant curvature. The same four states (the CT state c $^3B_2$ in $Pt(thpy)_2$ corresponds to d $^3B_2$ in $Pd(thpy)_2$, because MC and CT states are switched; see Tables 4 and 5) cause even more trouble in $Pd(thpy)_2$, where both their weights and energies only stabilize at an applied level shift of 0.3 au. To keep the applied level shift as low as possible, we therefore decided to apply a level shift of 0.2 au for all excited states except for these four, where instead 0.3 au was used for both complexes. These are the final results reported in Tables 4 and 5. Note, however, that all energy curves for A_1 and B_2 states with CT or LC character have pretty large slopes, thus afflicting the reported CASPT2 results for these states with a considerable uncertainty. An alternative choice might have been to apply a constant level shift of 0.3 au for all states. Just as an example, this would have increased the reported CASPT2 result for the lowest a $^3A_1$ state from 18 168 cm^{-1} (Table 5) to 18 690 cm^{-1} in $Pt(thpy)_2$, and from 19 689 cm^{-1} (Table 4) to 20 309 cm^{-1} in $Pd(thpy)_2$. These uncertainties have to be added to the expected errors in the CASPT2 results connected with the use of a limited number of active thpy π valence orbitals (see section 3.2), bringing the error bars on the reported CASPT2 excitation energies in Tables 4 and 5 to at least a few thousand cm^{-1}.

References and Notes

(1) Maestri, M.; Balzani, V.; Deuschel-Cornioley, C.; von Zelewsky, A. *Adv. Photochem.* **1992**, *17*, 1.
(2) Yersin, H.; Huber, P.; Wiedenhofer, H. *Coord. Chem. Rev.* **1994**, *132*, 35.
(3) Yersin, H.; Schützenmeier, S.; Wiedenhofer, H.; von Zelewsky, A. *J. Phys. Chem.* **1993**, *97*, 13496.
(4) Schmidt, J.; Wiedenhofer, H.; von Zelewsky, A.; Yersin, H. *J. Phys. Chem.* **1995**, *99*, 226.
(5) Wiedenhofer, H.; Schützenmeier, S.; von Zelewsky, A.; Yersin, H. *J. Phys. Chem.* **1995**, *99*, 13385.
(6) Becker, D.; Yersin, H.; von Zelewsky, A. *Chem. Phys. Lett.* **1995**, *235*, 490.
(7) Glasbeek, M.; Sitters, R.; van Veldhoven, E.; von Zelewsky, A.; Humbs, W.; Yersin, H. *Inorg. Chem.* **1998**, *37*, 5159.
(8) Yersin, H.; Humbs, W.; Strasser, J. In *Electronic and Vibronic Spectra of Transition Metal Complexes II*; Yersin, H., Ed.; *Topics in Current Chemistry*; Springer, Berlin, 1997; Vol. 191, pp 153−249.
(9) Vanhelmont, F. W. M.; Güdel, H. U.; Förtsch, M.; Bürgi, H. B. *J. Phys. Chem. A* **1997**, *101*, 2946.
(10) Vanhelmont, F. W. M.; Güdel, H. U.; Förtsch, M.; Bürgi, H. B. *Inorg. Chem.* **1997**, *36*, 5512.

(11) Maestri, M.; Sandrini, D.; Balzani, V.; Chassot, L.; Jolliet, P.; von Zelewsky, A. *Chem. Phys. Lett.* **1985**, *122*, 375.

(12) Maestri, M.; Sandrini, D.; Balzani, V.; von Zelewsky, A.; Jolliet, P. *Helv. Chim. Acta* **1988**, *71*, 134.

(13) Andersson, K.; Malmqvist, P.-Å.; Roos, B. O.; Sadlej, A. J.; Wolinski, K. *J. Phys. Chem.* **1990**, *94*, 5483.

(14) Pierloot, K.; Praet, E. V.; Vanquickenborne, L. G.; Roos, B. O. *J. Phys. Chem.* **1993**, *97*, 12220.

(15) Pierloot, K.; Tsokos, E.; Vanquickenborne, L. G. *J. Phys. Chem.* **1996**, *100*, 16545.

(16) Roos, B. O.; Andersson, K.; Fülscher, M. P.; Malmqvist, P.-Å.; Serrano-Andrés, L.; Pierloot, K.; Merchán, M. In *Advances in Chemical Physics: New Methods in Computational Quantum Mechanics*; Prigogine, I., Rice, S. A., Eds.; John Wiley & Sons: New York, 1996; Vol. XCIII, p 219.

(17) Roos, B. O. *Acc. Chem. Res.* **1999**, *32*, 137−144.

(18) Roos, B. O.; Fülscher, M. P.; Malmqvist, P.-Å.; Merchán, M.; Serrano-Andrés, L. In *Quantum Mechanical Electronic Structure Calculations with Chemical Accuracy*; Langhoff, S. R., Ed.; Kluwer Academic Publishers: Dordrecht, The Netherlands, 1995; p 357.

(19) Merchán, M.; Serrano-Andrés, L.; Fülscher, M. P.; Roos, B. O. In *Recent Advances in Multireference Methods*; Hirao, K., Ed.; World Scientific Publishing Co. Pte. Ltd.: P.O.B. 128, Farrer Road, Singapore, 1999; Vol. 4.

(20) Becke, A. D. *Phys. Rev. A* **1988**, *38*, 3098.

(21) Perdew, J. P. *Phys. Rev. B* **1986**, *33*, 8822.

(22) Ahlrichs, R.; Bär, M.; Häser, M.; Kölmel, C. *Chem. Phys. Lett.* **1989**, *162*, 165.

(23) Andrae, D.; Haeussermann, U.; Dolg, M.; Stoll, H.; Preuss, H. *Theor. Chim. Acta* **1990**, *77*, 123.

(24) Andersson, K.; Blomberg, M. R. A.; Fülscher, M. P.; Karlström, G.; Lindh, R.; Malmqvist, P.-Å.; Neogrády, P.; Olsen, J.; Roos, B. O.; Sadlej, A. J.; Schütz, M.; Seijo, L.; Serrano-Andrés, L.; Siegbahn, P. E. M.; Widmark, P.-O. *MOLCAS Version 4.1*; Department of Theoretical Chemistry, Chemistry Center, University of Lund: P.O.B. 124, S-221 00 Lund, Sweden, Lund, 1998.

(25) Barandiaran, Z.; Seijo, L.; Huzinaga, S. *J. Chem. Phys.* **1990**, *93*, 5843.

(26) Casarrubios, M.; Seijo, L. *J. Chem. Phys.* **1999**, *110*, 784.

(27) Pierloot, K.; Dumez, B.; Widmark, P.-O.; Roos, B. O. *Theor. Chim. Acta* **1995**, *90*, 87.

(28) Roos, B. O.; Andersson, K. *Chem. Phys. Lett.* **1995**, *245*, 215.

(29) Roos, B. O.; Andersson, K.; Fülscher, M. P.; Serrano-Andrés, L.; Pierloot, K.; Merchán, M.; Molina, V. *THEOCHEM* **1996**, *388*, 257.

(30) Malmqvist, P. Å.; Roos, B. O. *Chem. Phys. Lett.* **1989**, *155*, 189−194.

(31) Throughout this work, singlet excited states are counted with capital letters A, B, C ..., triplet states with small letters a, b, c, ..., according to an increasing CASPT2 energy. The counting is done per symmetry representation. The (singlet) ground state is denoted with an X.

(32) van Gisbergen, S. J. A.; Groeneveld, J. A.; Rosa, A.; Snijders, J. G.; Baerends, E. J. *J. Phys. Chem. A* **1999**, *103*, 6835.

(33) Balzani, V.; Maestri, M.; Melandri, A.; Sandrini, D.; Chassot, L.; Cornioley-Deuschel, C.; Jolliet, P.; Maeder, U.; von Zelewsky, A. In *Photochemistry and Photophysics of Coordination Compounds*; Yersin, H., Vogler, A., Eds.; Springer-Verlag: Berlin Heidelberg New York, 1987; p 71.

(34) Lever, A. B. P. *Inorganic Electronic Spectroscopy*. Elsevier: Amsterdam, 1984.

(35) Barigelletti, F.; Sandrini, D.; Maestri, M.; Balzani, V.; von Zelewsky, A.; Chassot, L.; Jolliet, P.; Maeder, U. *Inorg. Chem.* **1988**, *27*, 3644.